



Galactic halo bubble magnetic fields and UHECRs

Vasundhara Shaw, Andrew Taylor, Arjen Van Vliet

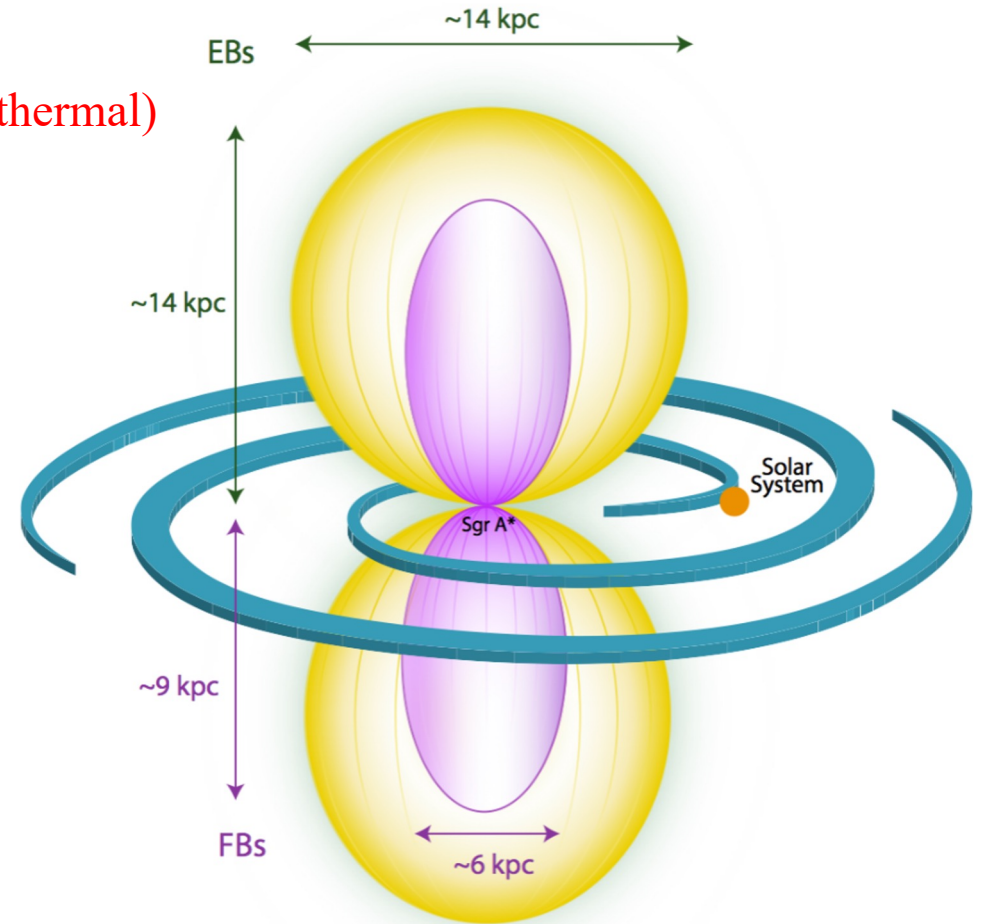
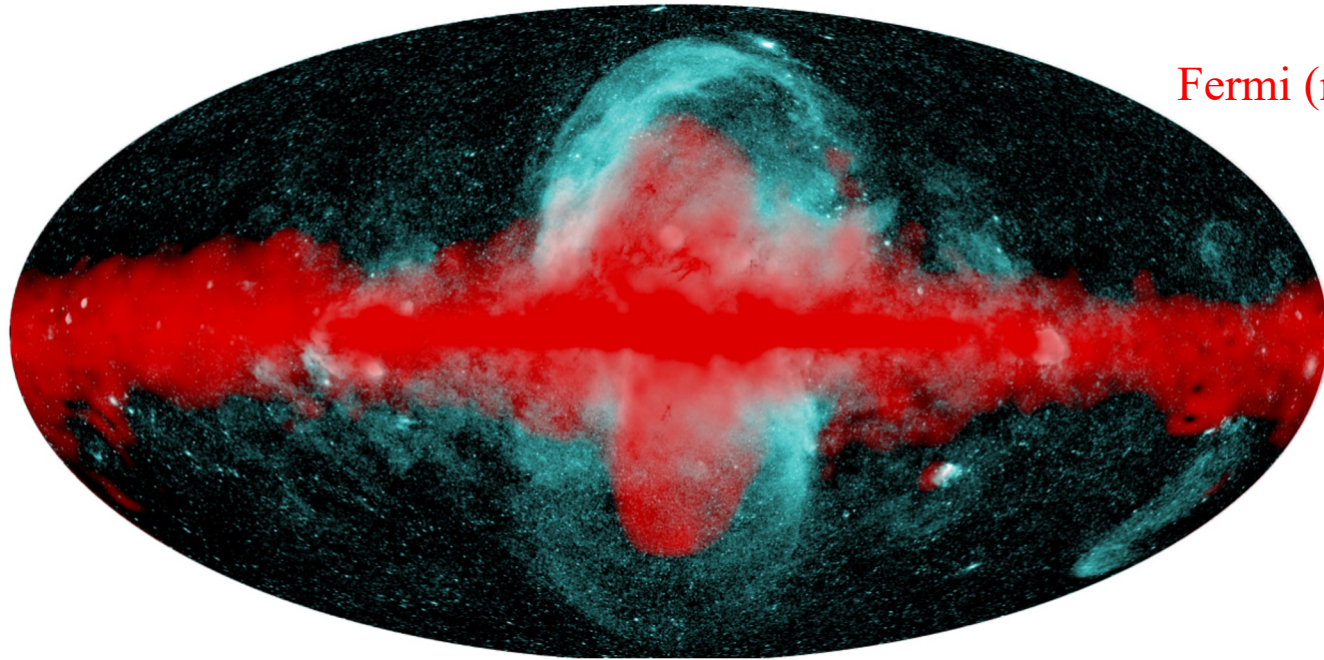
1) <https://www.cosmos.esa.int/web/planck/picture-gallery>

2) Predehl, P., Sunyaev, R.A., Becker, W. et al. Detection of large-scale X-ray bubbles in the Milky Way halo. Nature 588, 227–231 (2020).⁰

Galactic Halo Bubbles

eRosita (thermal)

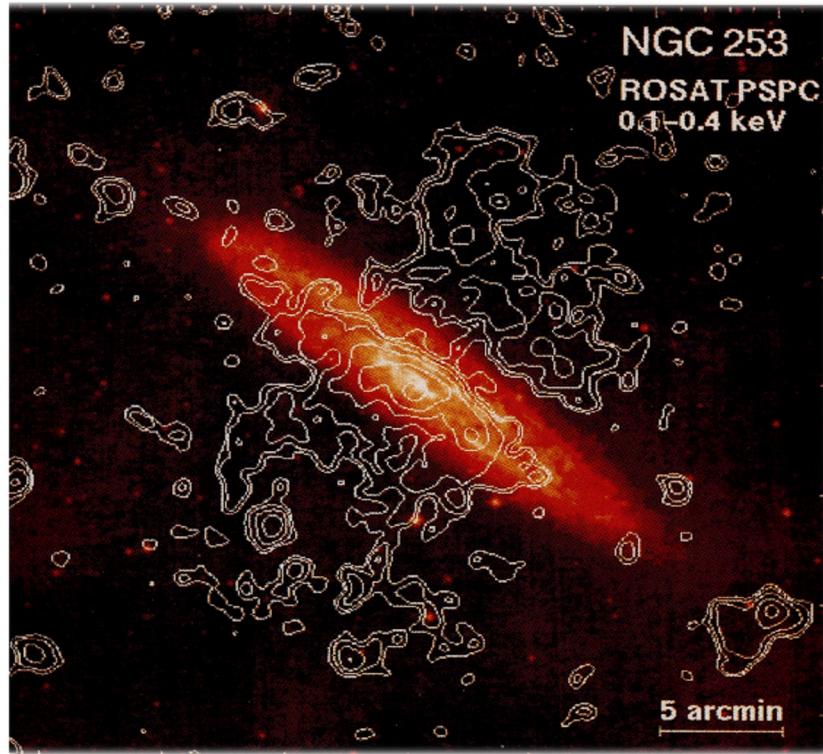
Fermi (non-thermal)



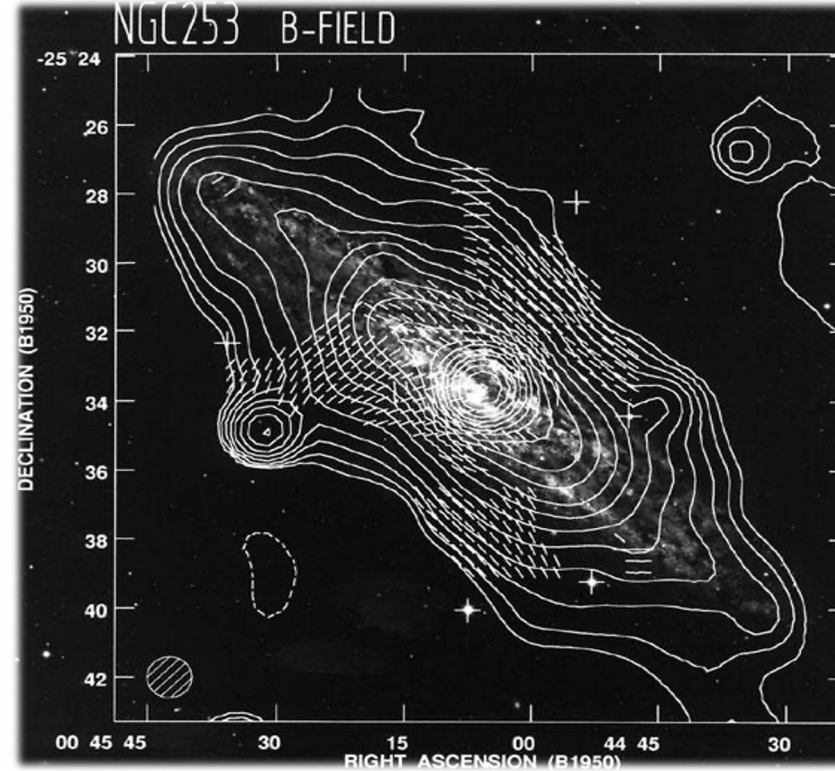
10^{56} erg in X-rays
 Total energy 10^{54-55} erg in disc

Large scale structures = large scale fields

(Pietsch et.al 1996)

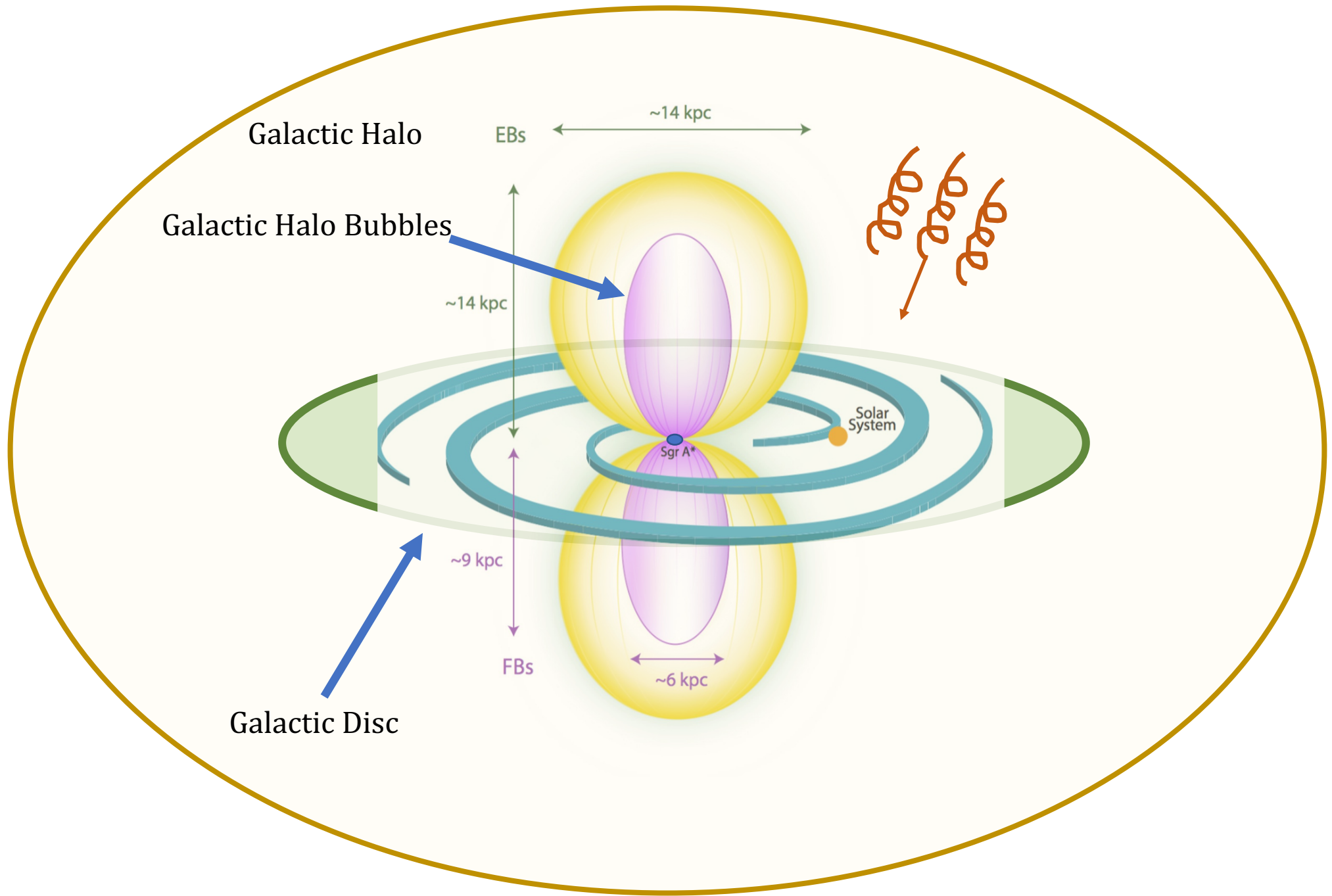


(Beck et.al 1994)



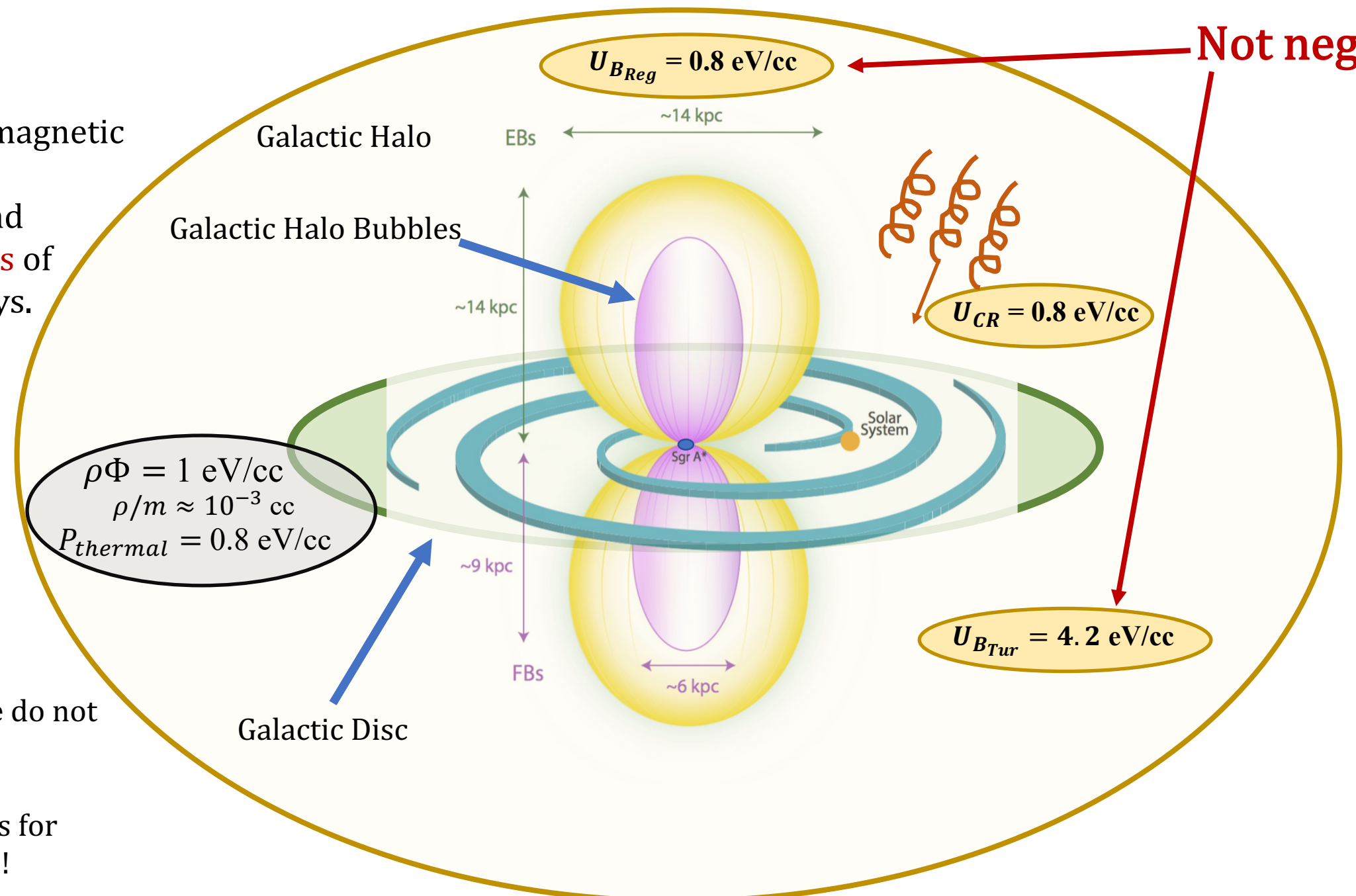
Total radio intensity (*contours*) and magnetic field orientation of [NGC 253](#).

Milky way is not a starburst galaxy yet it has outflow!



We need magnetic fields to understand deflections of cosmic rays.

Note: We do not have any accurate estimates for the Halo !



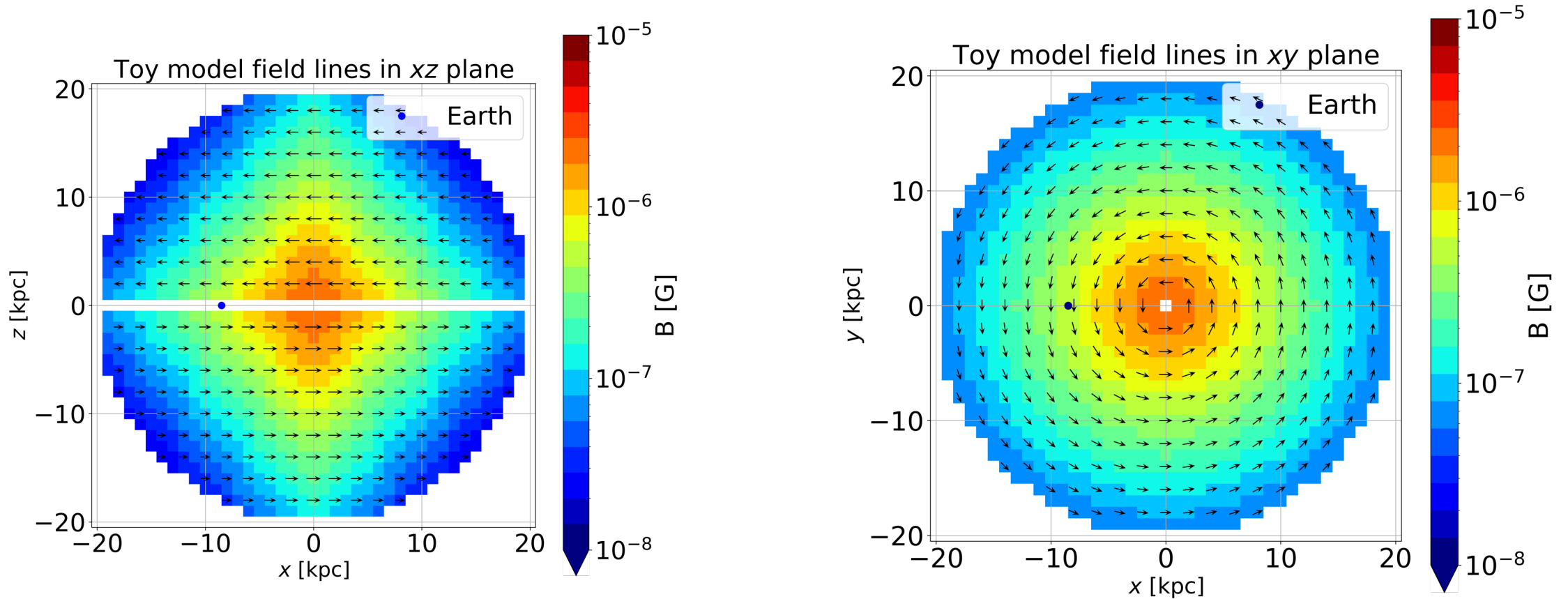
Not negligible!

Probing magnetic fields with synchrotron radiation



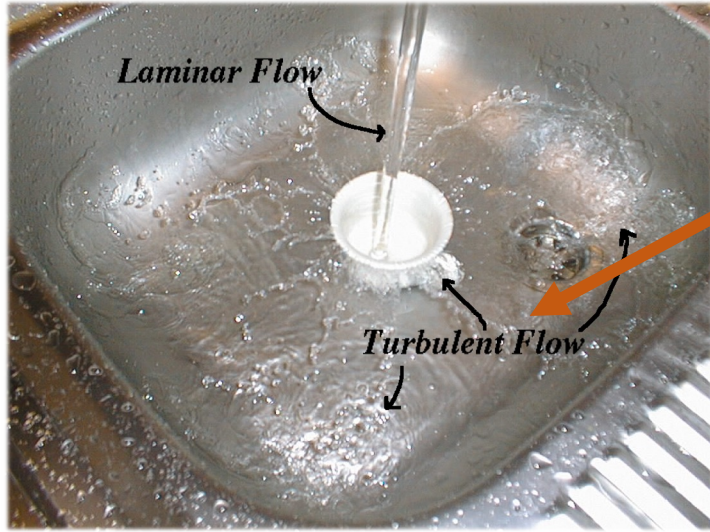
Toy Model – Structured fields

$$B_{\text{tor}} = B_{\text{str}} e^{(-|z|/Z_{\text{mag}})} e^{(-z_{\text{min}}/|z|)} e^{(-|r|/R_{\text{mag}})}$$



$$R_{\text{mag}} \ \& \ Z_{\text{mag}} = 5 \text{ kpc and } 6 \text{ kpc } B_{\text{str}} = 3.96 \ \mu\text{G}$$

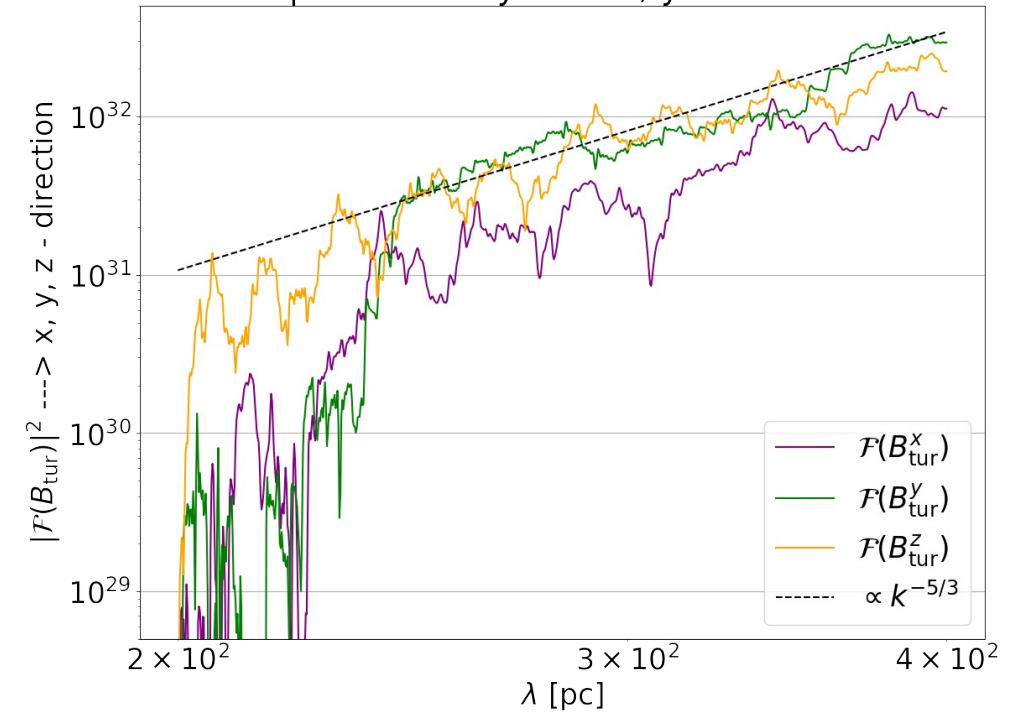
Toy Model – Turbulent fields



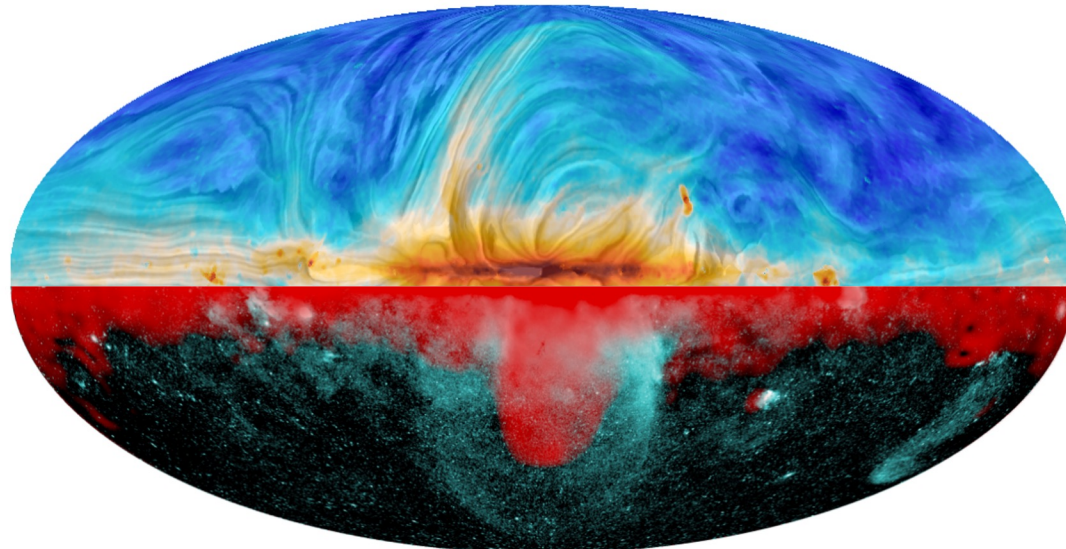
Outflow induces turbulent fields

$\frac{5}{3}$ Kolmogorov spectrum for turbulent fields

Power spectral analysis in x, y and z directions



Almost same power in each mode



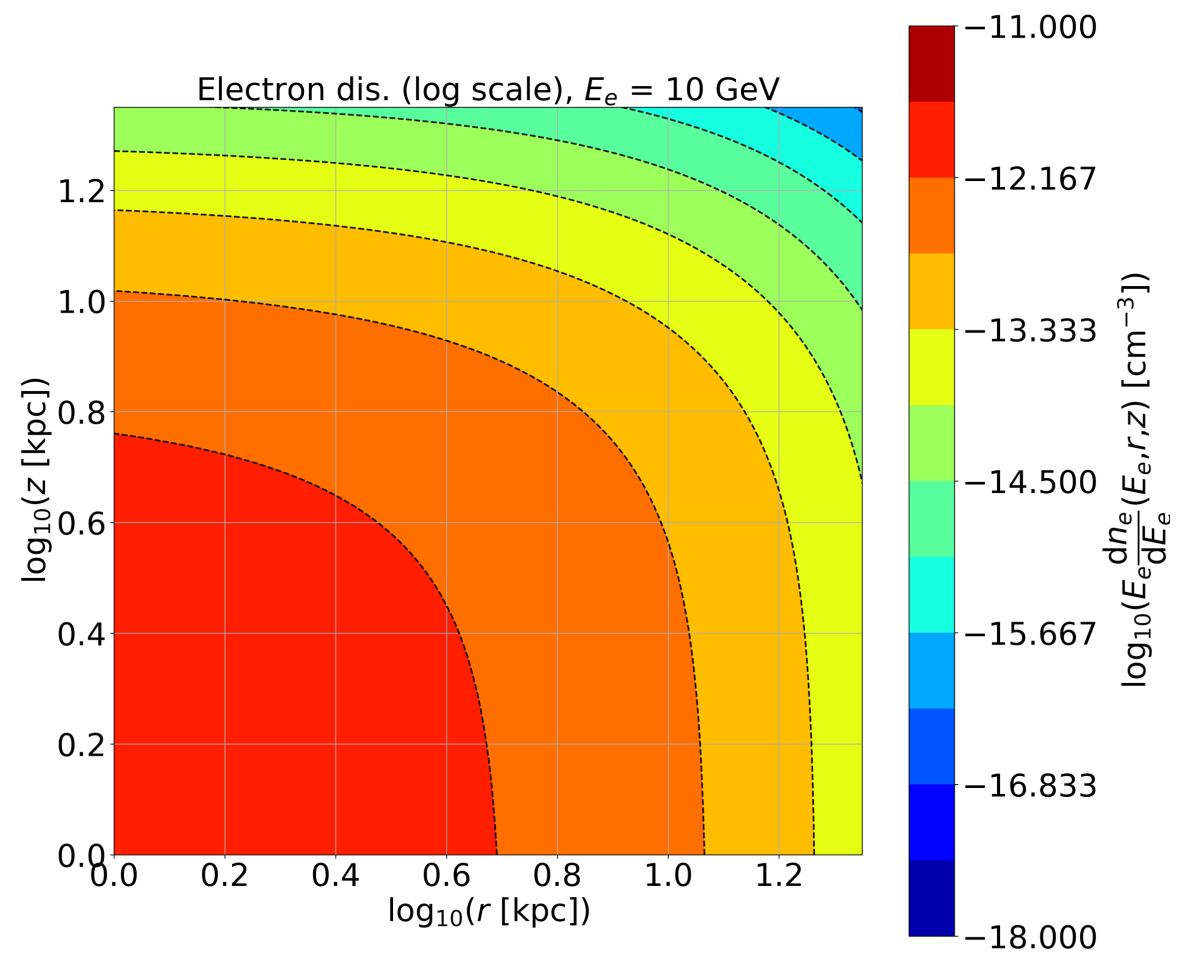
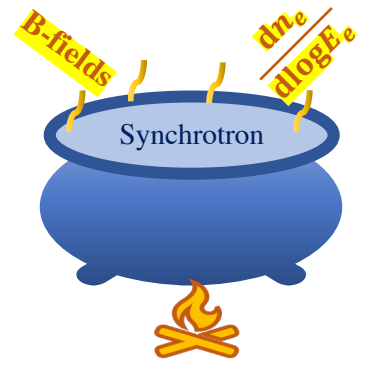
1) <https://www.cosmos.esa.int/web/planck/picture-gallery>

2) Predehl, P., Sunyaev, R.A., Becker, W. et al. Detection of large-scale X-ray bubbles in the Milky Way halo. Nature 588, 227–231 (2020).

Toy Model – non-thermal electron distribution at 10 GeV

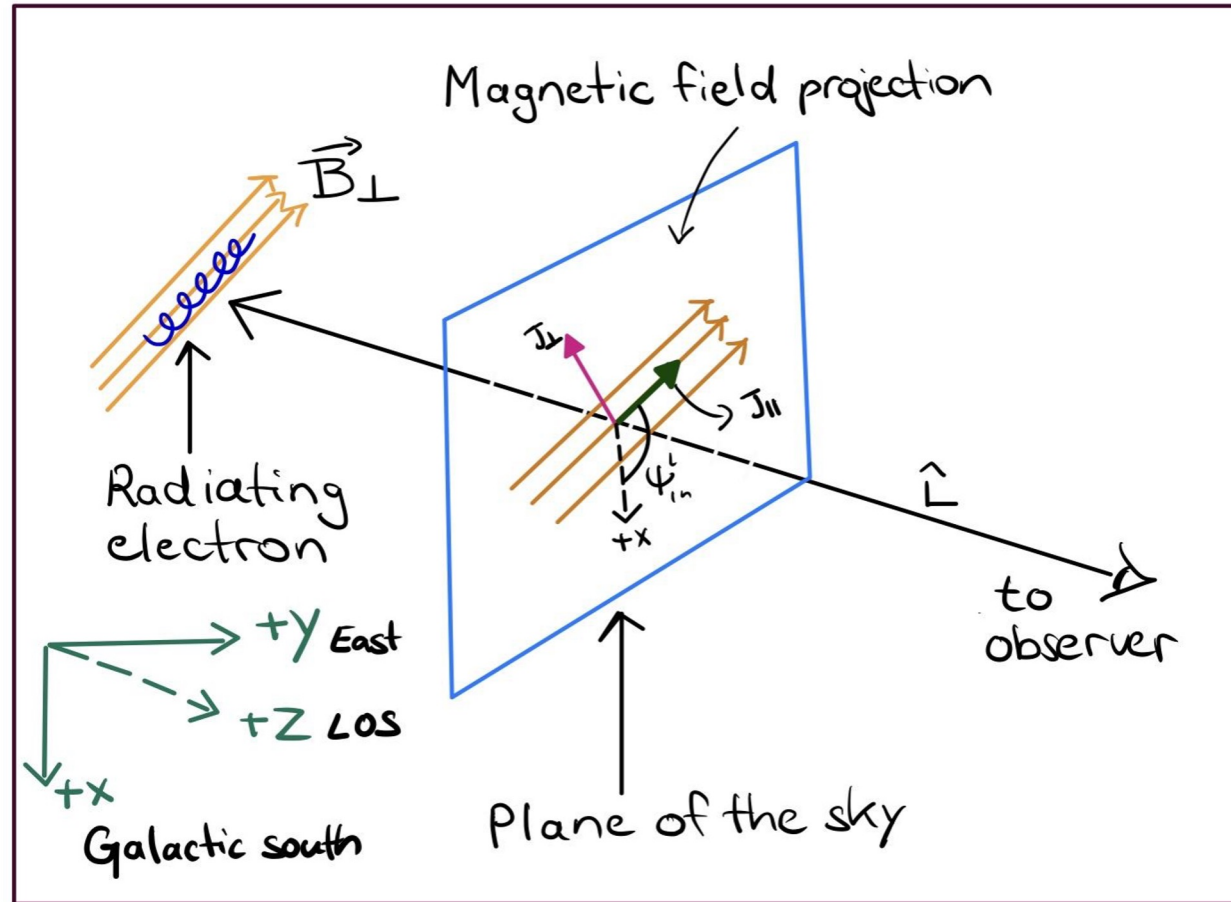
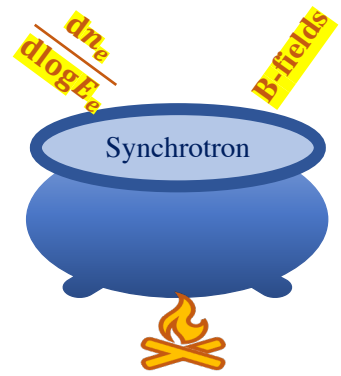
$$\frac{dn_e}{d\log E_e} = C_{\text{norm}} \left(\frac{E_e}{E_{10\text{GeV}}} \right)^{-p+1} e^{-r/R_{\text{el}}} \text{sech}^2 \left(\frac{z}{Z_{\text{el}}} \right)$$

Together magnetic fields and non-thermal electrons give Synchrotron!

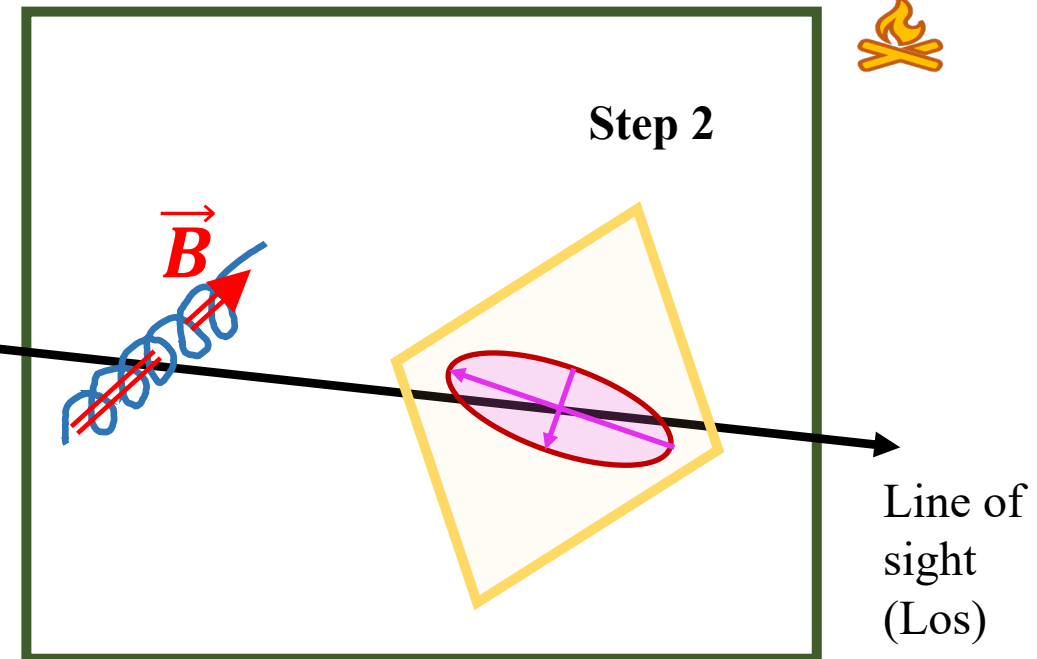
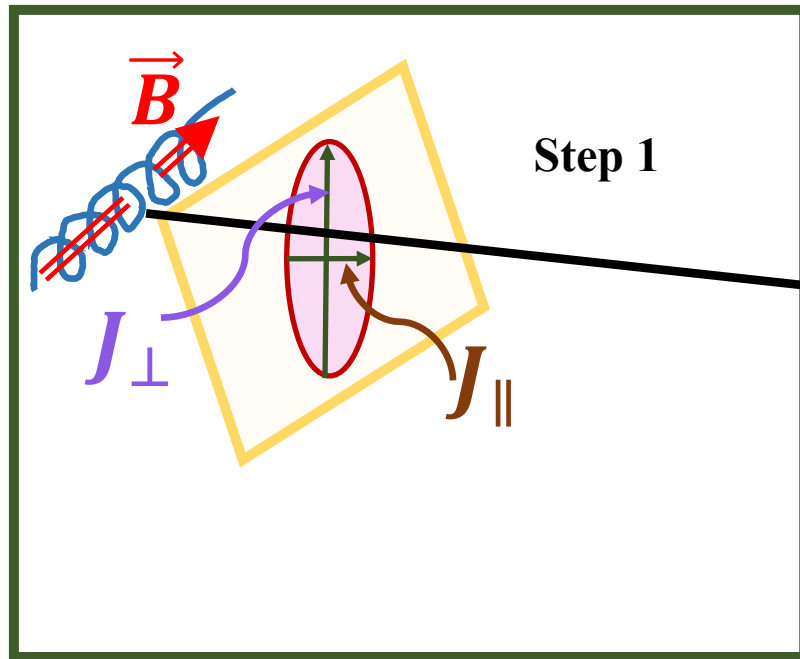
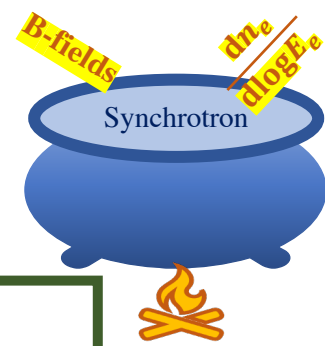


$R_{\text{el}} \ \& \ Z_{\text{el}} = 5 \text{ kpc} \ \text{and} \ 6 \text{ kpc}$

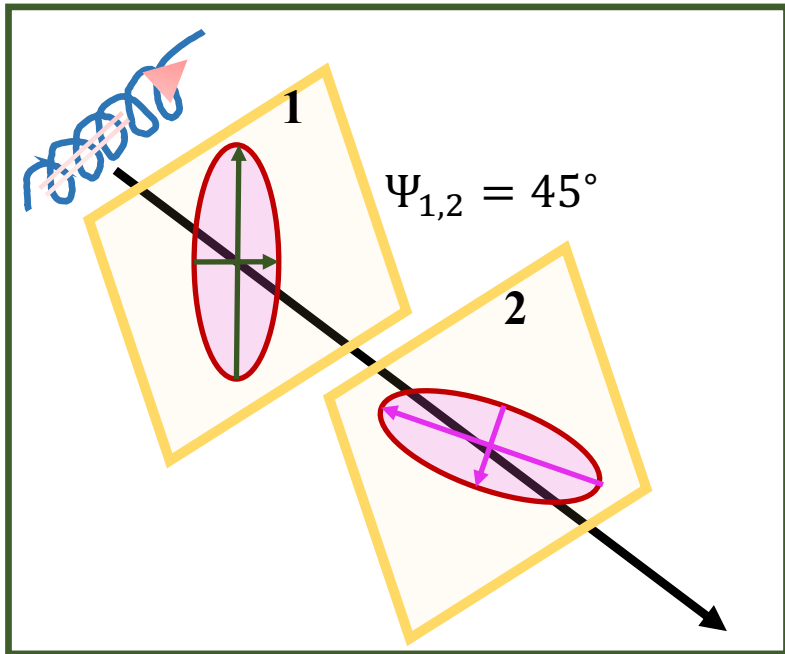
Synchrotron radiation – standard picture



Synchrotron radiation – emission ellipses

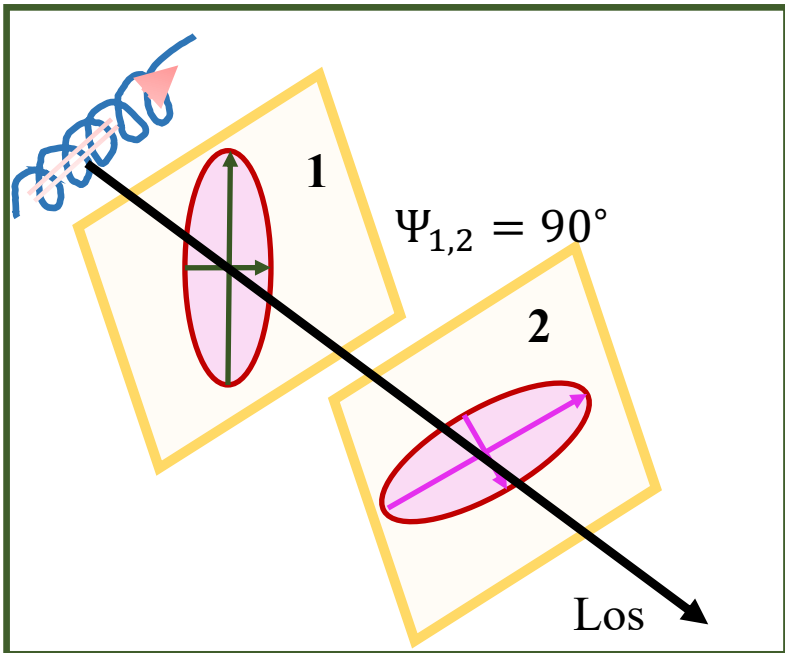


Synchrotron radiation



Polarised synchrotron

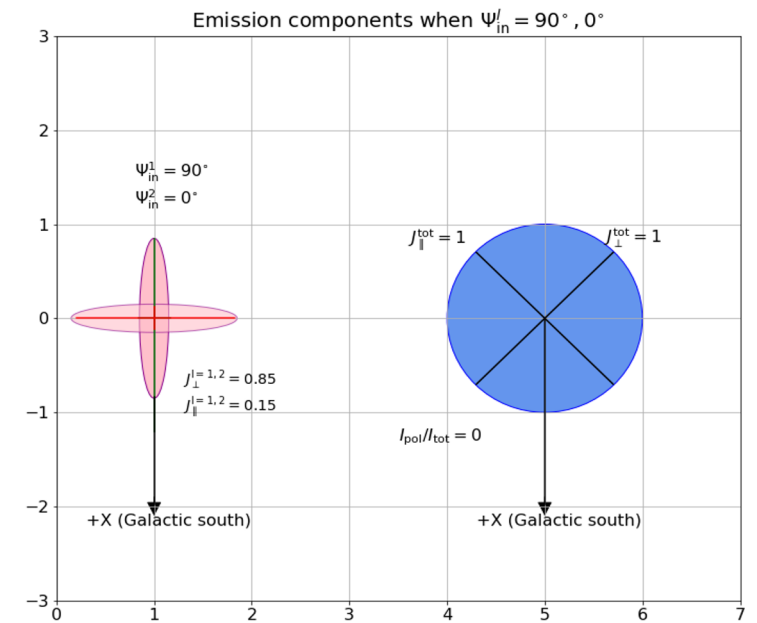
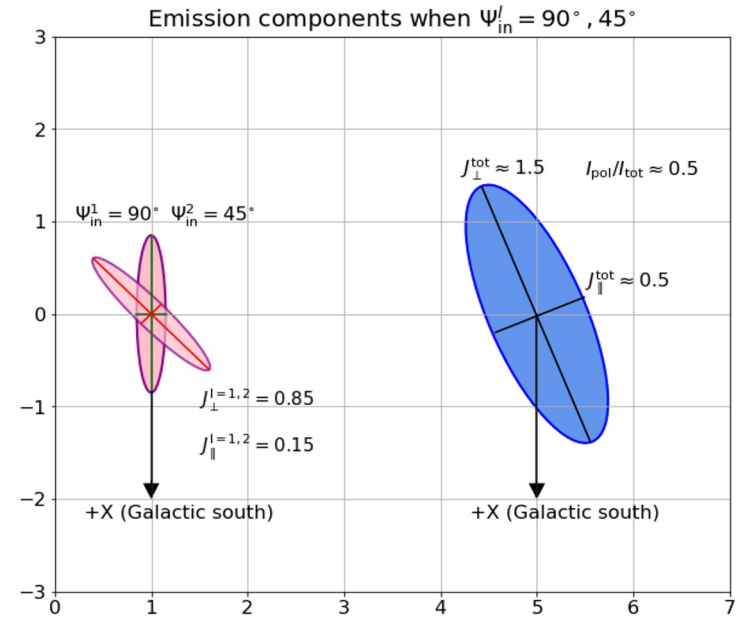
Probes magnetic field strength and geometry



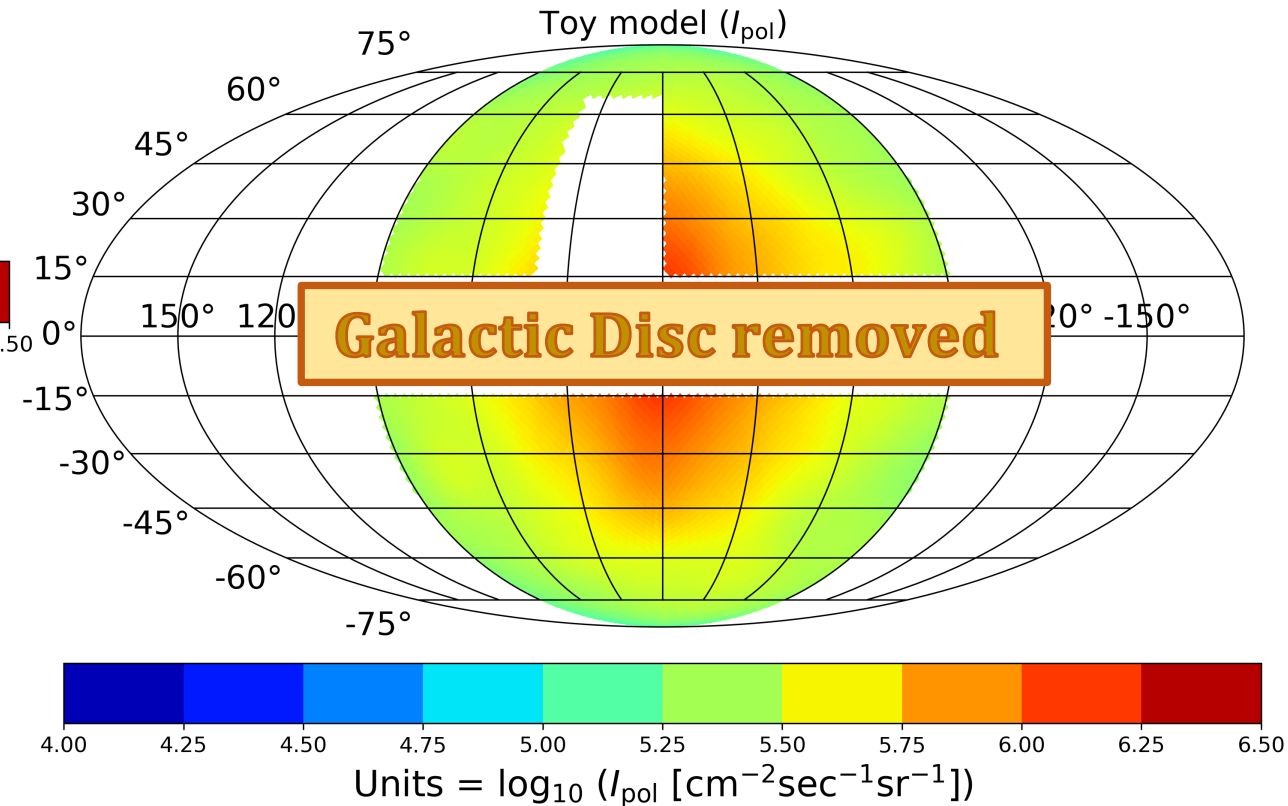
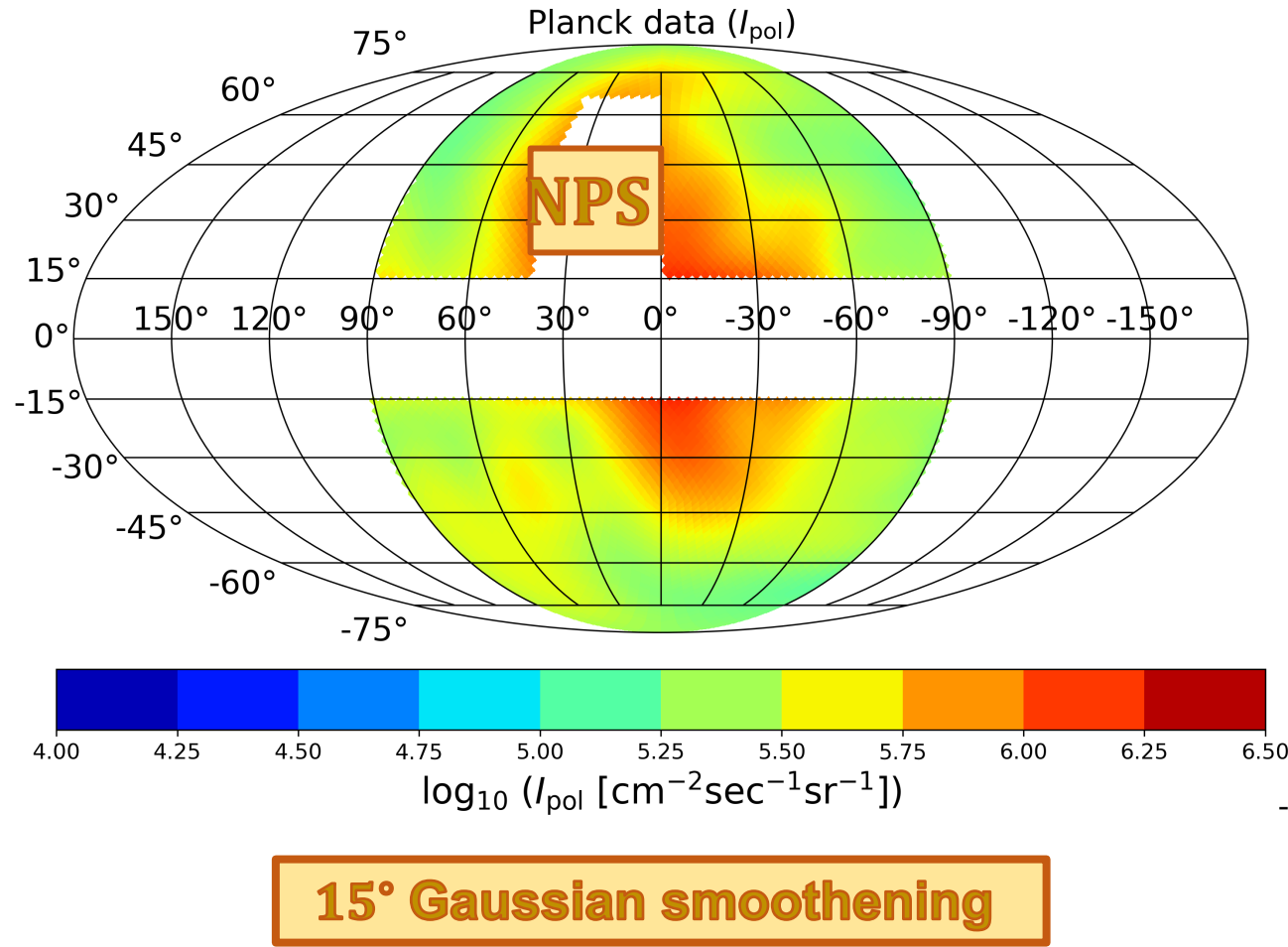
Unpolarised synchrotron

Probes magnetic field strength only

Maximum emission is observed when the electron pitch angles are perpendicular to magnetic fields.

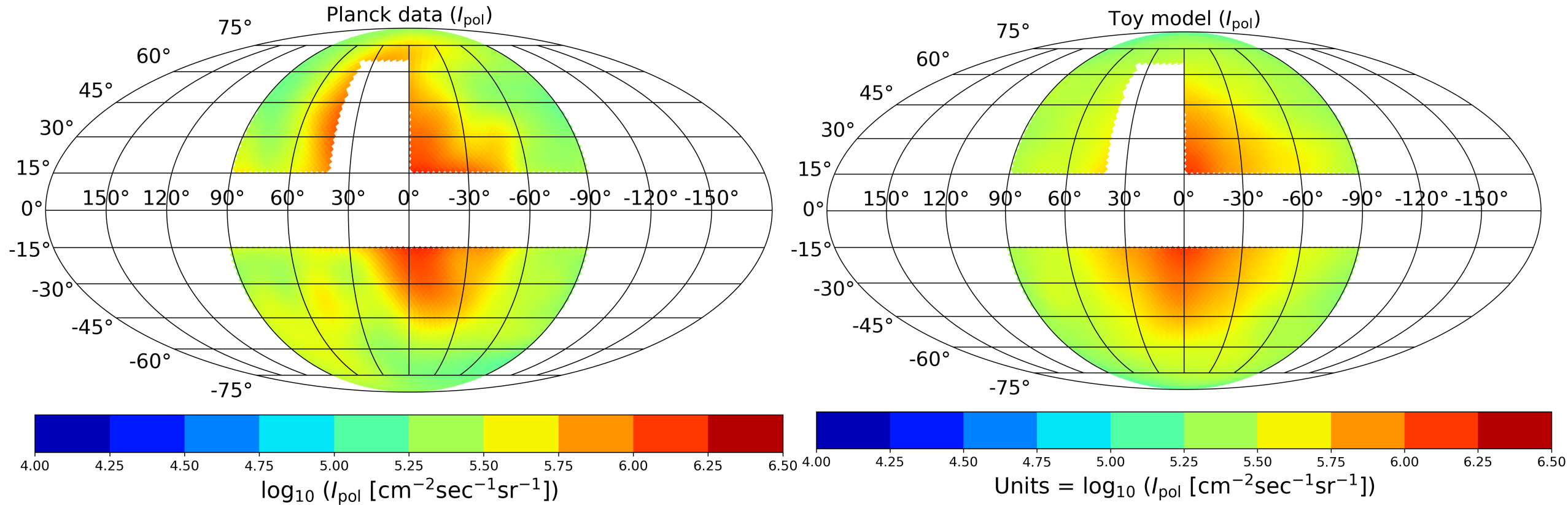


Results – Best fit case

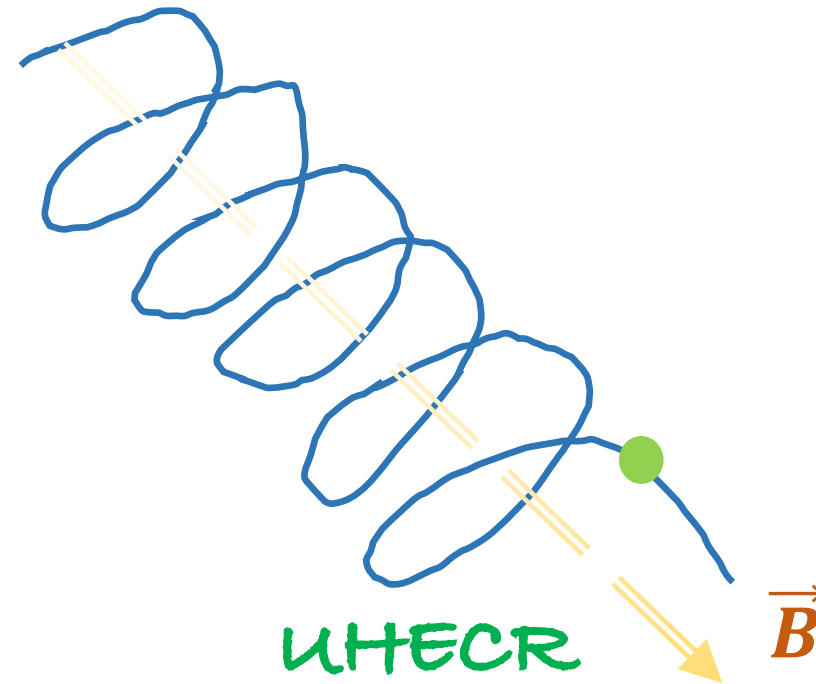


Constraints

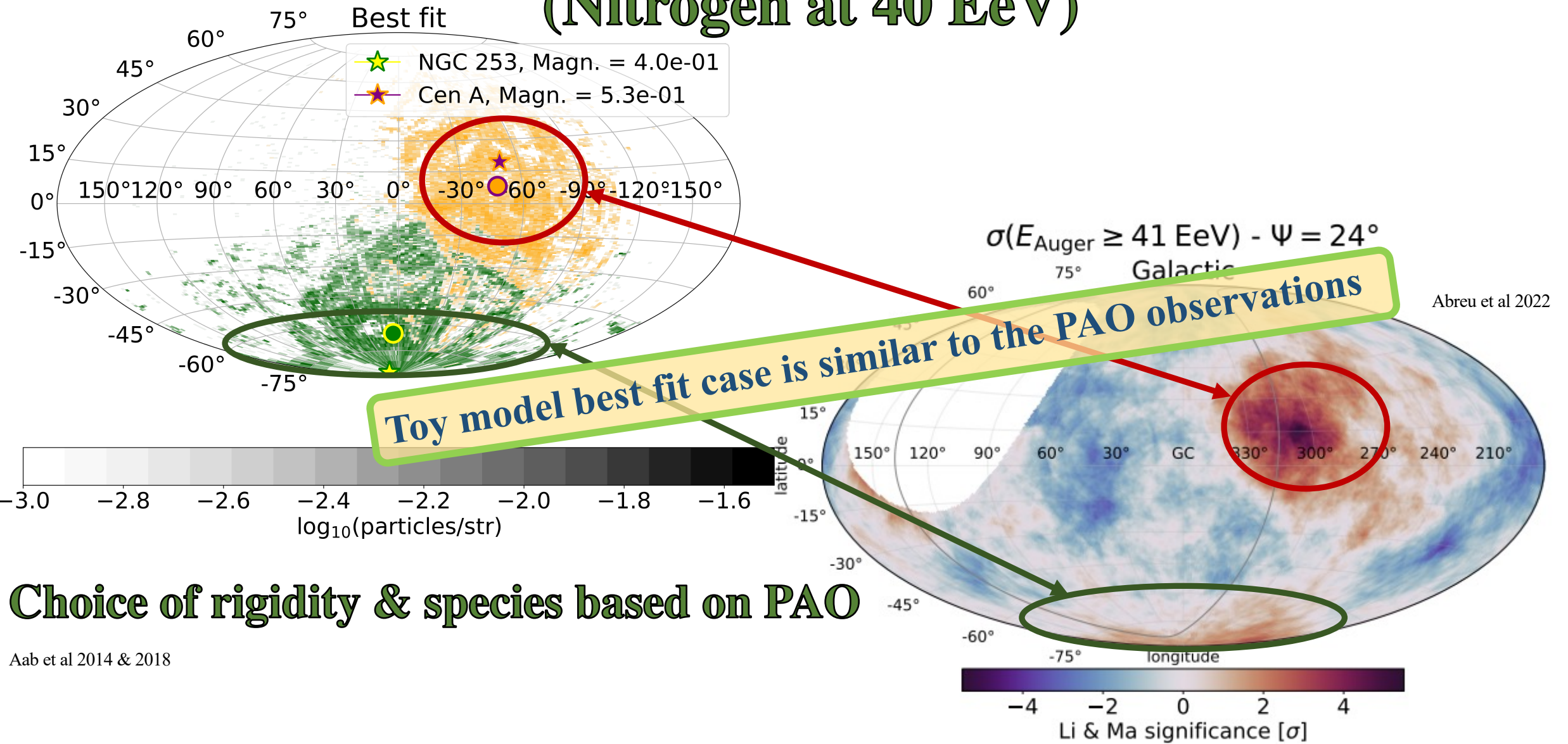
Best-fit value with 1σ constraint		
Parameter	Best-fit value	Description
B_{str}	$3.96^{+6.63}_{-1.96} \mu\text{G}$	Structured field strength
B_{tur}	$6.72^{+9.97}_{-3.56} \mu\text{G}$	Turbulent field strength
$R_{\text{Mag}} = R_{\text{el}}$	5^{+1}_{-0}kpc	Radial cut off
$Z_{\text{Mag}} = Z_{\text{el}}$	6^{+1}_{-0}kpc	Azimuthal cut off
$\log_{10} (C_{\text{norm}} [\text{cm}^{-3}])$	$-11.72^{+0.62}_{-0.93}$	Electron density at 10 GeV



Backtracking of UHECRs through toy model using CRPropa3



Arrival directions of UHECRs – Toy Model vs Auger (Nitrogen at 40 EeV)

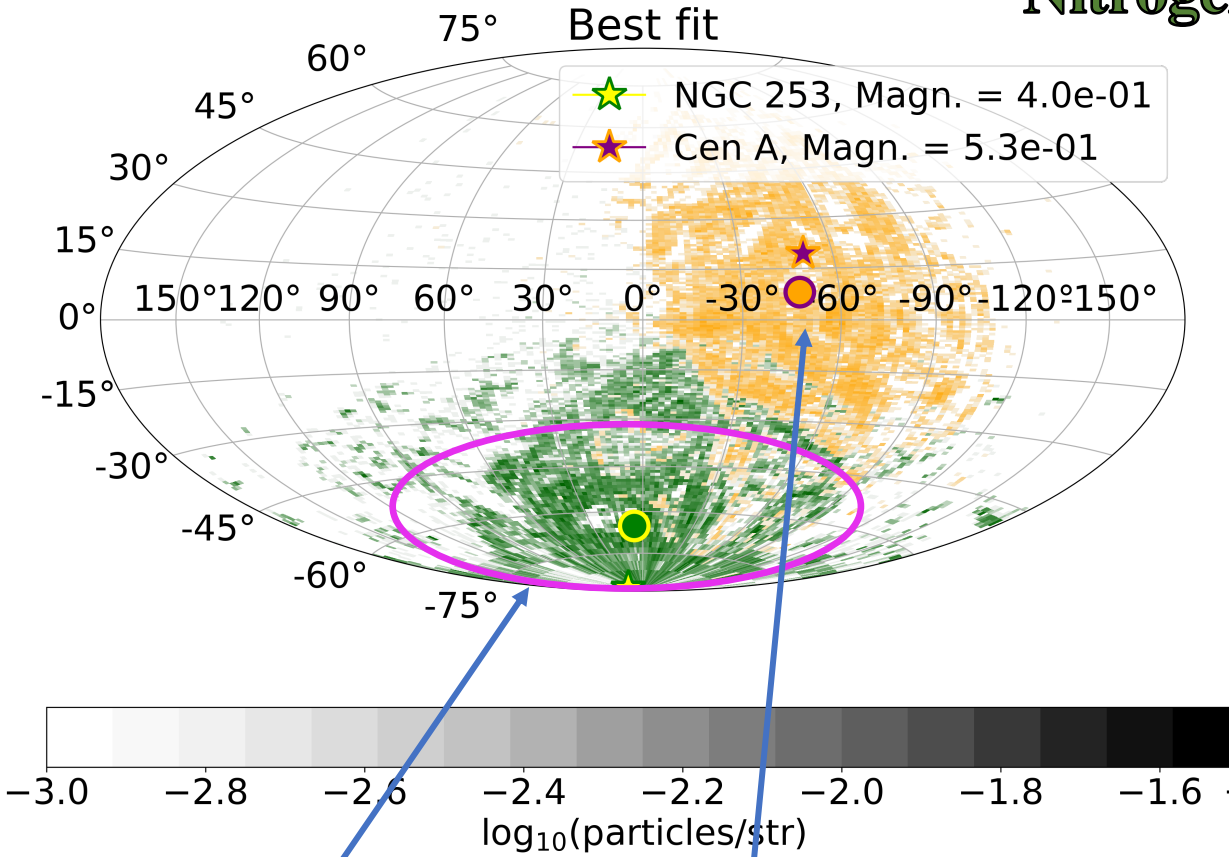
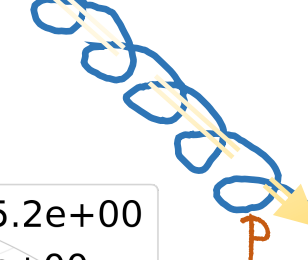


Choice of rigidity & species based on PAO

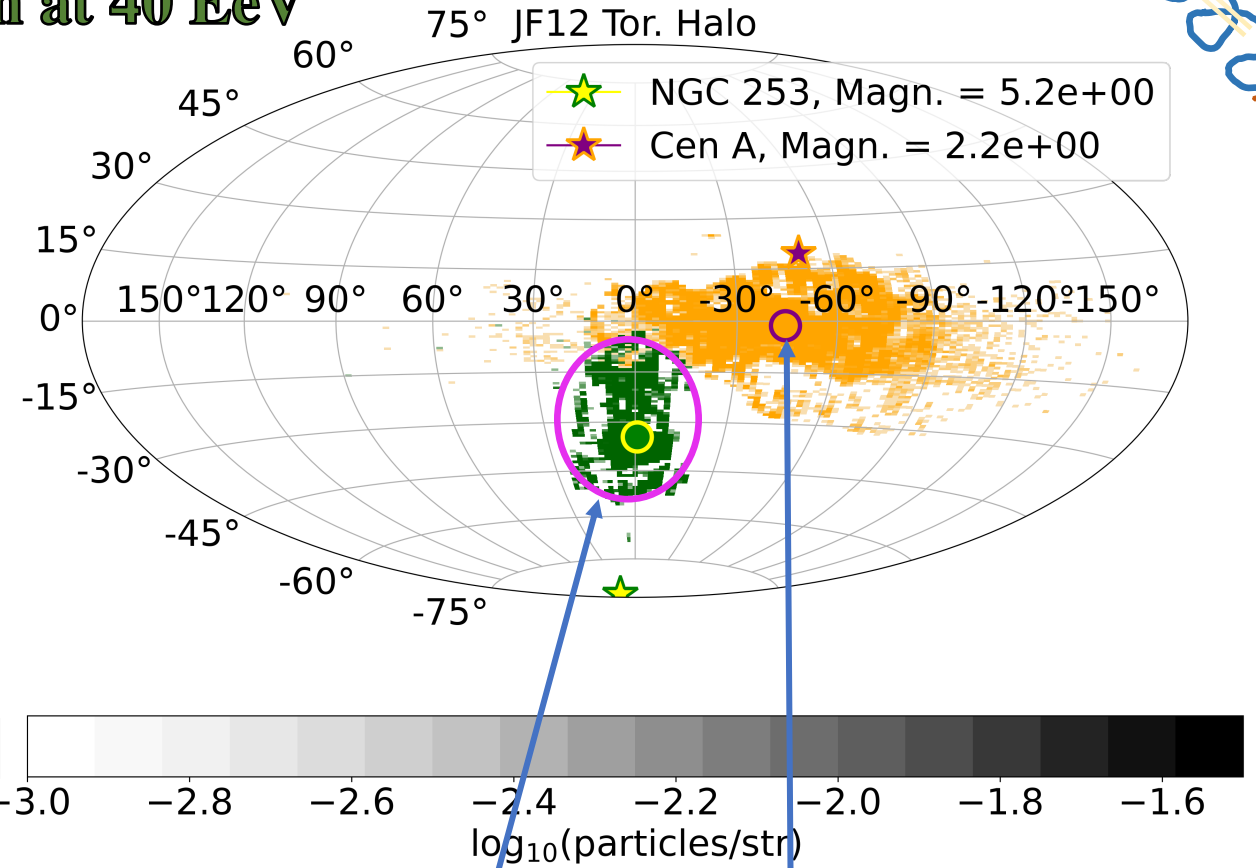
Aab et al 2014 & 2018

Toy Model vs JF12 Torroidal Halo

Nitrogen at 40 EeV



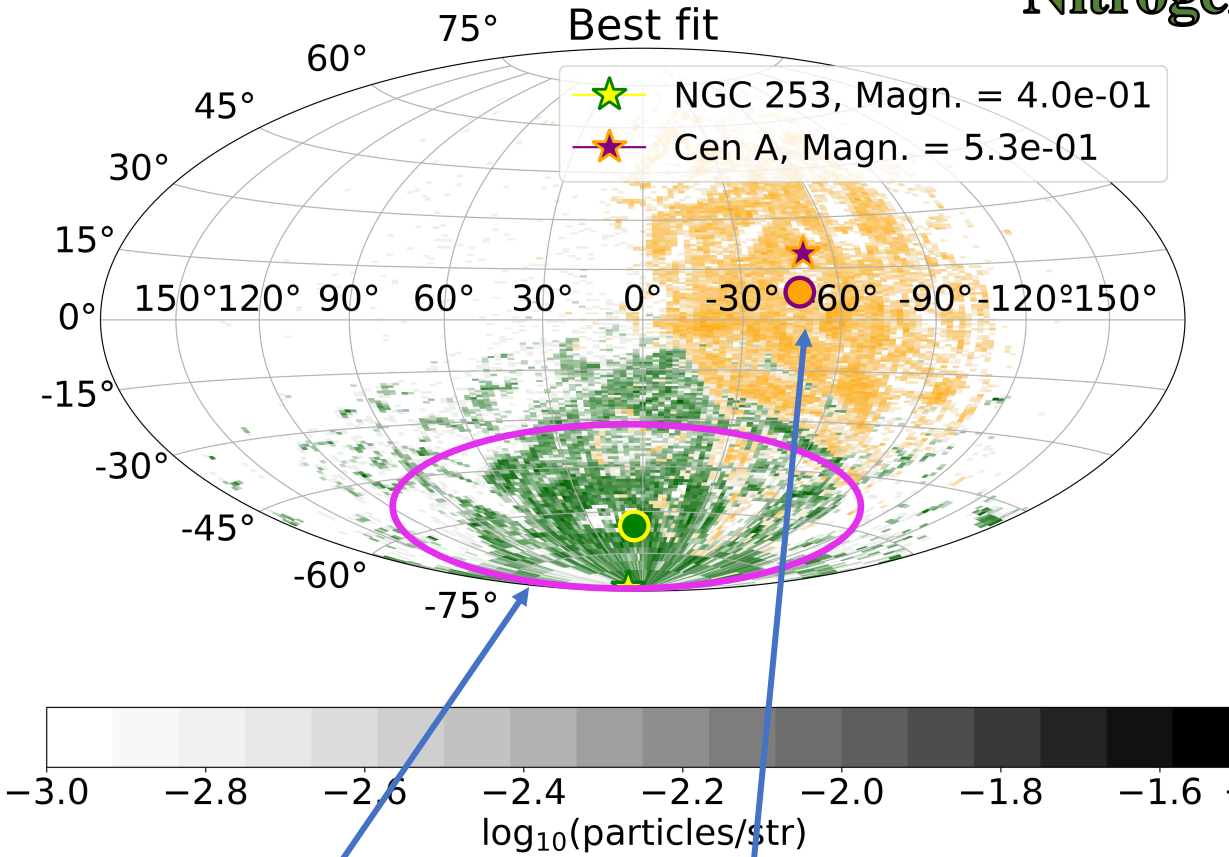
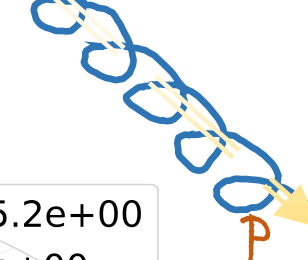
$$\sigma_{\text{NGC 253}} = 32^\circ, \sigma_{\text{Cen A}} = 33^\circ$$



$$\sigma_{\text{NGC 253}} = 9^\circ, \sigma_{\text{Cen A}} = 22^\circ$$

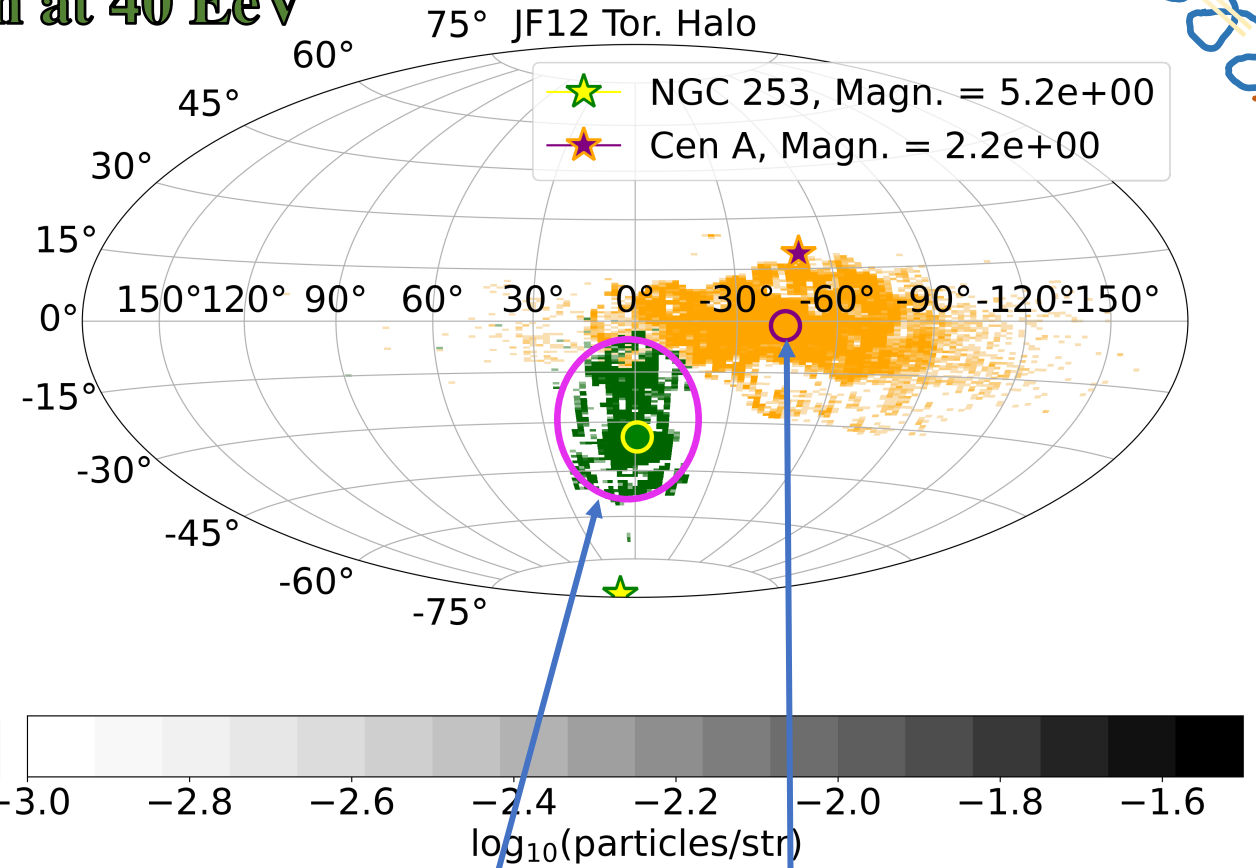
Toy Model vs JF12 Torroidal Halo

Nitrogen at 40 EeV



$$\sigma_{\text{NGC 253}} = 32^\circ, \sigma_{\text{Cen A}} = 33^\circ$$

Structured fields - Overall coherent deflection
Turbulent fields - Spreading out the directions of the particle deflections around this overall deflected direction



$$\sigma_{\text{NGC 253}} = 9^\circ, \sigma_{\text{Cen A}} = 22^\circ$$

Spreading Effect - Toy model 5-10 times larger than JF12
Deflections are dominated by halo NOT disc

Conclusions & Outlook

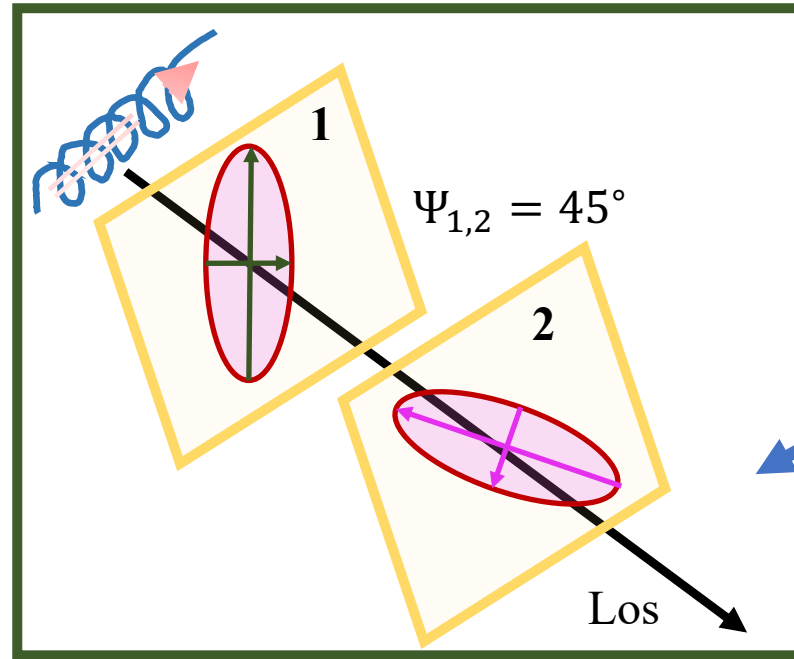
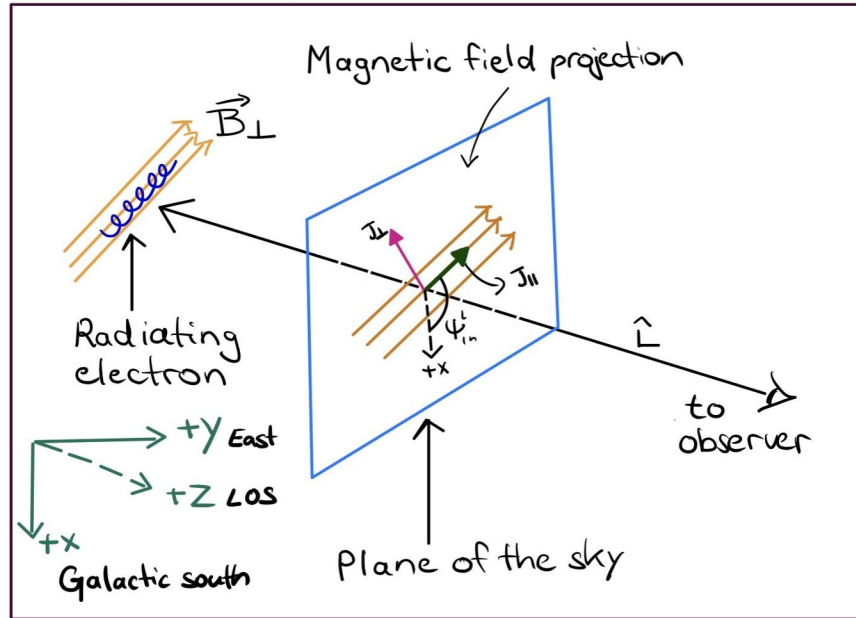
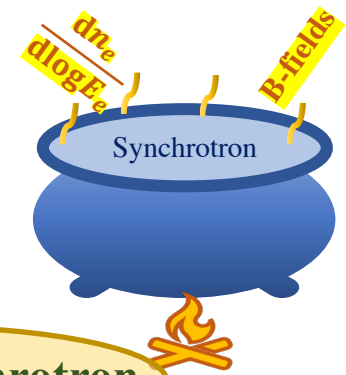
- Our results indicate $\sim 7 \mu\text{G}$ total fields over a large spatial extent with the height of halo being $\sim 6 \text{ kpc}$ in z-direction which is compatible with S-PASS and other observations.
- Arrival direction of cosmic rays is highly tangled with both the structured and turbulent magnetic fields. We find the cosmic ray deflections from our model are similar with NGC 253 and Cen A hotspots from Auger (Abreu et al. 2022).
- Rotation measures from extra-galactic sources like FRBs should be factored in once the MeerKat and FAST data is public.
- C-BASS, Quijote and Lofar data can also be useful for studying the halo at different frequencies in the future.



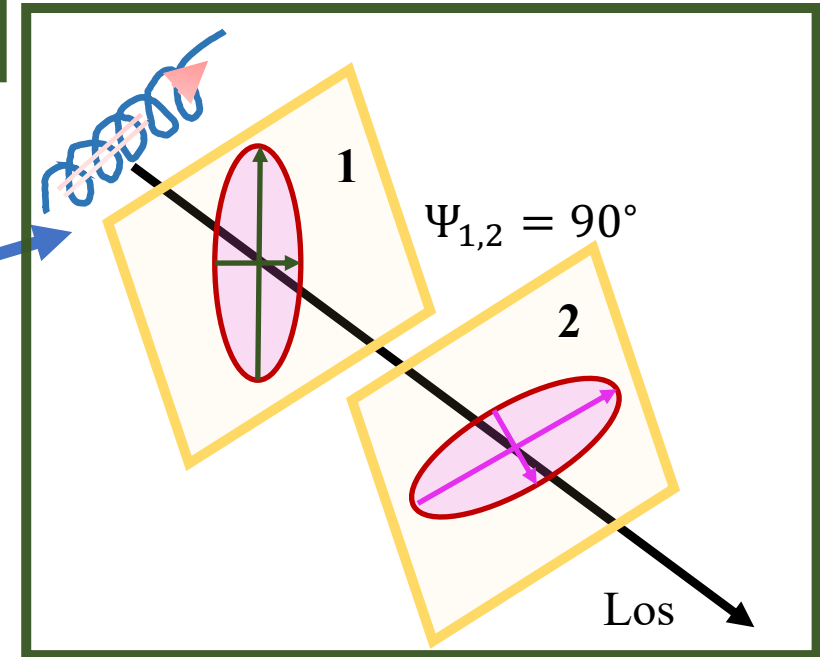
Extras



Synchrotron radiation – emission ellipses



Polarised synchrotron

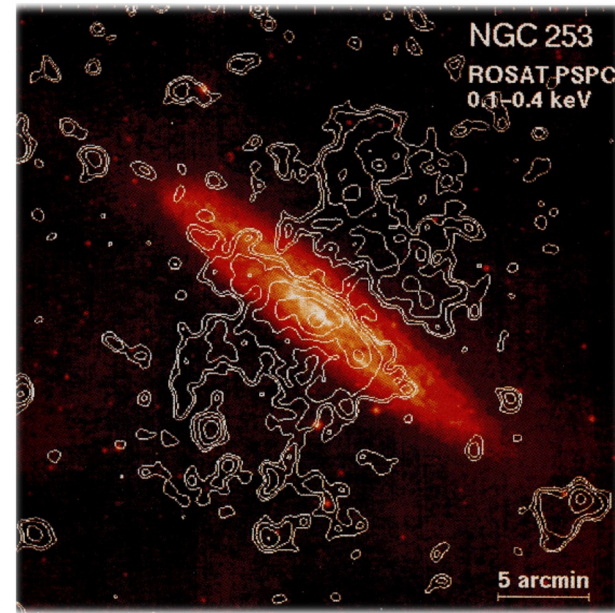


Unpolarised synchrotron

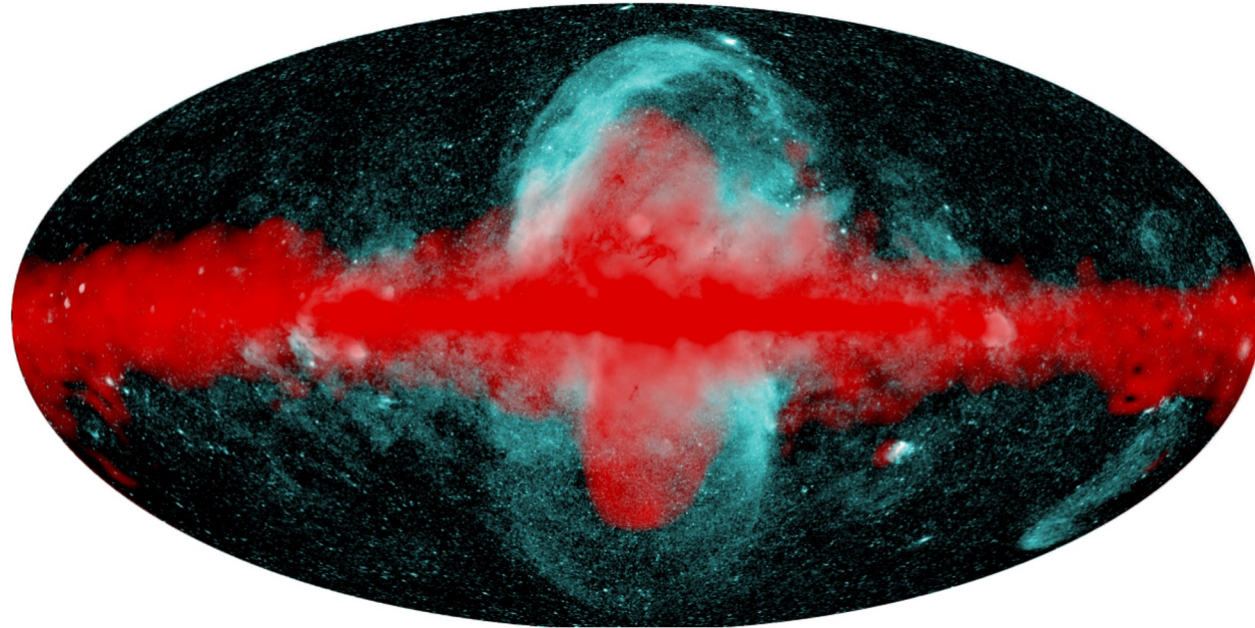
Maximum emission is observed when the electron pitch angles are perpendicular to magnetic fields

Milky way is not a starburst galaxy yet it has outflow!

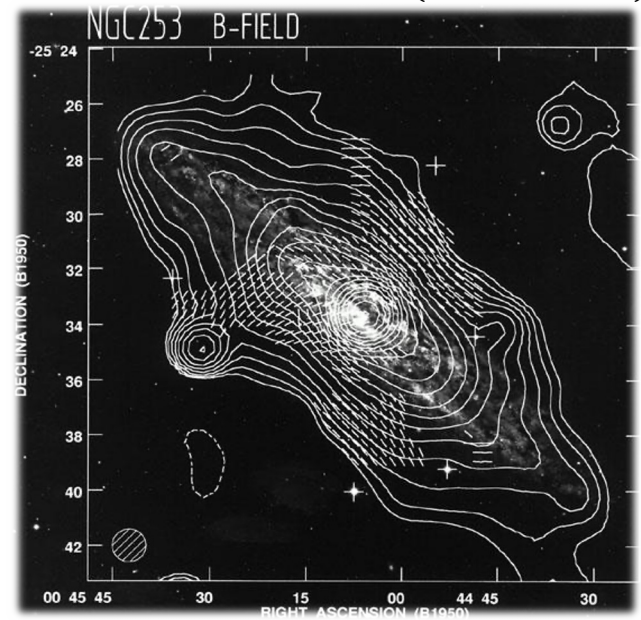
(Pietsch et.al 1996)



Outflows as seen in starburst galaxies!



(Beck et.al 1994)



Large scale structures imply large scale magnetic fields

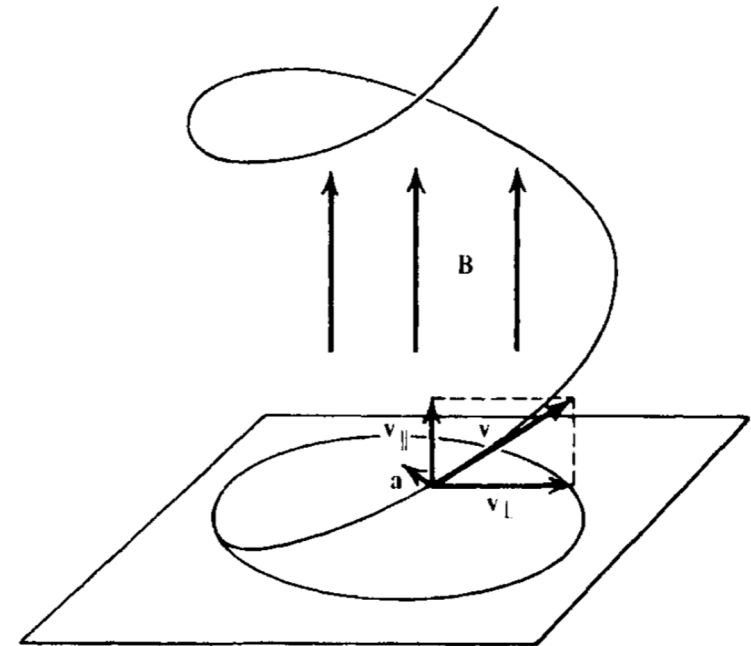
Total radio intensity (*contours*) and magnetic field orientation of [NGC 253](#).

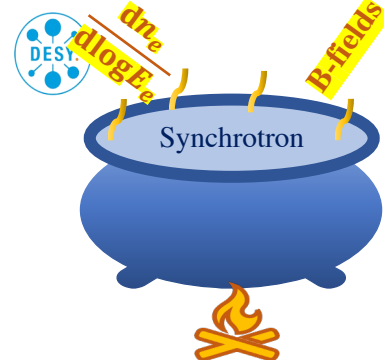
SYNCHROTRON RADIATION

- "Magneto-bremsstrahlung" = Radiation emitted by relativistic charged particles (mostly electrons) due to acceleration ("gyro-motion") in a static magnetic field.

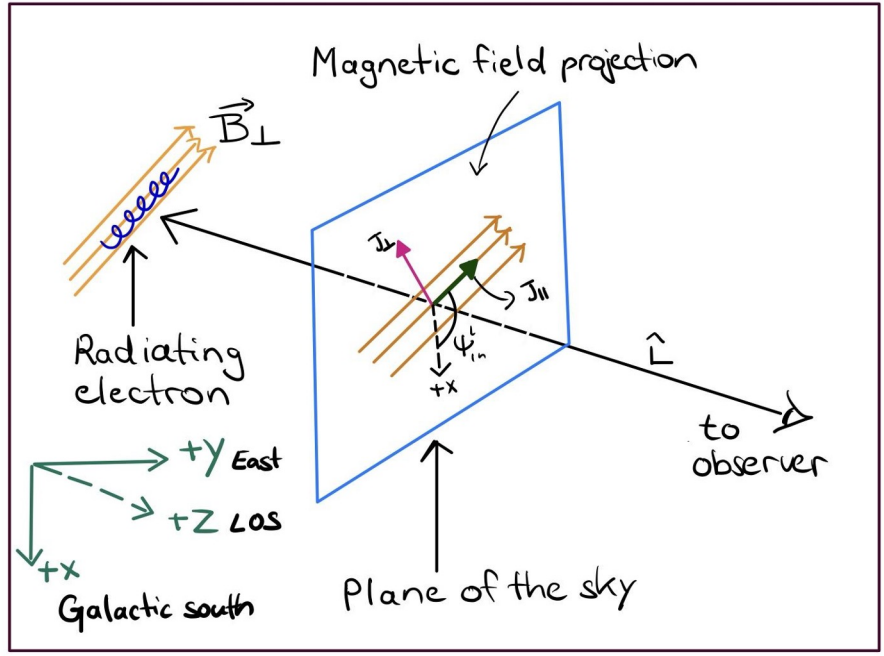
$$\langle P_{syn} \rangle = \frac{4}{3} c \sigma_T \beta^2 \gamma^2 u_B \propto \gamma^2 B^2$$

- u_B : magnetic energy density $\left(\frac{B^2}{8\pi}\right)$
- $\beta\gamma$: speed of electron
- σ_T : Thompson scattering





Polarised synchrotron radiation



$$J_{\perp}^l = \frac{1}{\tau} \int_{\log E_e^{\min}}^{\log E_e^{\max}} \frac{dn_e}{d\log E_e} d\log E_e \left[F\left(\frac{E_{\gamma}}{E_{\gamma}^{\text{peak}}}\right) + G\left(\frac{E_{\gamma}}{E_{\gamma}^{\text{peak}}}\right) \right] \quad (3)$$

and

$$J_{\parallel}^l = \frac{1}{\tau} \int_{\log E_e^{\min}}^{\log E_e^{\max}} \frac{dn_e}{d\log E_e} d\log E_e \left[F\left(\frac{E_{\gamma}}{E_{\gamma}^{\text{peak}}}\right) - G\left(\frac{E_{\gamma}}{E_{\gamma}^{\text{peak}}}\right) \right] \quad (4)$$

where

$$\tau^{-1} = \frac{\sqrt{3}\alpha}{4\pi} \frac{B_{\perp}}{B_{\text{crit}}} \frac{m_e c^2}{\hbar}, \quad E_{\gamma}^{\text{peak}} = \frac{3}{2} \Gamma_e^2 \frac{B_{\perp}}{B_{\text{crit}}} m_e c^2,$$

and

$$F(x) = x \int_x^{\infty} K_{5/3}(x') dx', \quad G(x) = x K_{2/3}.$$



Extras